BIOCHEMISTRY
including biophysical chemistry & molecular biology

Article

pubs.acs.org/biochemistry

GTP Regulates the Interaction between MciZ and FtsZ: A Possible Role of MciZ in Bacterial Cell Division

Shashikant Ray, Ashutosh Kumar, and Dulal Panda*

Department of Biosciences and Bioengineering, Indian Institute of Technology Bombay, Mumbai 400076, India

Supporting Information

ABSTRACT: MciZ, a peptide with 40 amino acid residues, has been shown to be expressed during bacterial sporulation, to inhibit Z-ring formation in bacteria, and to inhibit the assembly of FtsZ in vitro. Here, MciZ was found to bind to FtsZ in vitro with a dissociation constant of 0.3 ± 0.1 μM. Guanosine nucleotides inhibited the binding of MciZ to FtsZ; however, GTP inhibited the binding of MciZ to FtsZ more strongly than GDP. In addition, MciZ inhibited the binding of 2′,3′-*O*-(2,4,6-trinitrocyclohexadienylidene)-GTP, a fluorescent analogue of GTP, to FtsZ. The results indicated that MciZ shares its binding site on FtsZ with GTP. Furthermore, M19I, an N-terminal 19-residue peptide (MKVHRMPKGVVLVGKAWEI) of MciZ, inhibited the assembly and GTPase activity of FtsZ in vitro. The results suggested that GTP plays an important role in the regulation of the interaction between FtsZ and MciZ and that M19I may be used as a lead peptide to design peptide inhibitors of FtsZ assembly.

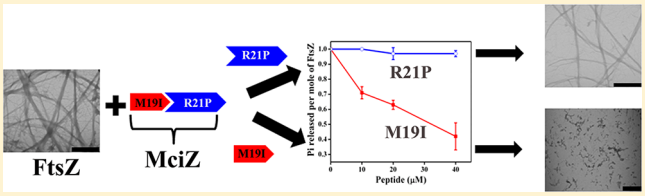

FtsZ monomers assemble to form a cytokinetic Z-ring at the midcell that engineers bacterial cell division.[1−4] The Z-ring is a highly dynamic structure that constantly exchanges subunits with the cytosol.[5,6] The assembly dynamics of FtsZ in the Z-ring is tightly regulated by the combined action of several accessory proteins, and a defect in the assembly or stability of the FtsZ filaments has been found to have a deleterious effect on bacterial cell division.[2,7−10] Several of these accessory proteins such as FtsA, SepF, and ZipA are known to enhance FtsZ assembly and to stabilize the Z-ring, while a group of proteins such as EzrA, SulA, MinCD, and MciZ are known to inhibit FtsZ assembly, thereby inhibiting Z-ring formation and functions.[2,11−13]

Recently, MciZ, a peptide with 40 amino acid residues, has been found to be expressed during sporulation in *Bacillus subtilis*.[14] MciZ and three other proteins (SpoIID, SpoIIM, and SpoIIP) inhibit the assembly of FtsZ in mother sporangia during sporulation. MciZ has been shown to inhibit FtsZ polymerization and to reduce the GTPase activity of FtsZ.[14] Interestingly, MciZ inhibits FtsZ assembly at low and moderate GTP concentrations.[14] Further, a substitution mutation near the GTP-binding pocket of FtsZ has been found to confer resistance to the inhibitory effect of MciZ, raising the possibility that GTP might occlude the binding of FtsZ to MciZ.[14] However, it still remains unclear how GTP modulates the binding of MciZ to FtsZ. In addition, the mechanism by which MciZ inhibits FtsZ polymerization and the site of interaction of MciZ with FtsZ are not known.

In this study, we sought to elucidate how GTP regulates the interaction of MciZ and FtsZ. The evidence presented in this work indicates that MciZ shares its binding site on FtsZ with GTP. Moreover, the heterologous expression of MciZ in *Escherichia coli* cells inhibited both Z-ring and cytokinesis in these cells. Further, we identified a region of MciZ that was found to be sufficient to inhibit the assembly and GTPase activity of FtsZ in vitro. The results provide insight into the mechanism by which MciZ inhibits the assembly of FtsZ and also improve our understanding of the cell division regulatory mechanism of MciZ. The identification of an active MciZ peptide will assist in the design of inhibitors of FtsZ assembly, which may have potential uses as antibacterial agents.

EXPERIMENTAL PROCEDURES

Materials. M19I and R21P peptides were purchased from USV-custom peptide synthesis (Mumbai, India). Pipes, BSA, lysozyme, GTP, DAPI, PMSF, FITC, and Cy3-conjugated goat anti-rabbit secondary antibody were purchased from Sigma (St. Louis, MO). TNP-GTP was purchased from Molecular Probes, Inc. (Eugene, OR). IPTG was obtained from Calbiochem. Ni-NTA resin was procured from Qiagen, and Bio-Gel-P6 resin was purchased from Bio-Rad. Rabbit polyclonal FtsZ antibody was developed by Bangalore Genei. All other reagents used were of analytical grade.

Isolation of *B. subtilis* FtsZ. *E. coli* BL21(DE3) pLysS cells transformed with vector pET16b carrying *B. subtilis ftsZ* were grown at 37 °C in LB medium in the presence of 12.5 μg/mL chloramphenicol and 100 μg/mL ampicillin.[8,11,15] Cells were induced (OD_{600} = 0.8) with 1 mM IPTG for 6 h and harvested by centrifugation. The pellet was washed with lysis buffer [50 mM NaH_2PO_4 (pH 8.0) and 300 mM NaCl], suspended in ice-cold lysis buffer containing 0.1% β-mercaptoethanol, 2 mM

Received: September 11, 2012
Revised: November 20, 2012
Published: December 13, 2012

PMSF, and 1 mg/mL lysozyme, and incubated for 1 h on ice. The cells were then disrupted by sonication (10 pulses for 30 s each), and the crude lysate obtained was cleared by centrifugation at 80000*g* and 4 °C. Imidazole (5 mM) was added to the cleared cell lysate to prevent nonspecific binding to Ni-NTA resin. Cell lysate was then mixed with Ni-NTA resin and incubated with gentle shaking for 1 h at 4 °C. The resin was loaded on the column, and the flow-through was collected. The column was extensively washed with wash buffer [25 mM Pipes (pH 6.8) and 300 mM NaCl] containing varying concentrations of imidazole (25, 50, and 100 mM). The protein was finally eluted with 25 mM Pipes buffer (pH 6.8) containing 250 mM imidazole. The protein was pooled and then desalted using the Biogel P-6 resin. The protein concentration was estimated by the Bradford method using bovine serum albumin as a standard protein.[16] The FtsZ concentration was adjusted using a correction factor of 1.2 for the FtsZ/BSA ratio.[17]

Isolation and Purification of MciZ. MciZ was expressed and purified as described previously.[14] Briefly, *E. coli* BL21 cells containing the His_6-MciZ construct were grown at 37 °C in LB medium in the presence of 50 μg/mL chloramphenicol and 30 μg/mL kanamycin. The cells were then induced (OD_{600} = 0.6) with 1 mM IPTG for 2 h. The cells were harvested and washed with lysis buffer [10 mM Tris-HCl (pH 8.0), 8 M urea, and 0.1 M NaH_2PO_4]. The cell pellet was resuspended in ice-cold lysis buffer containing 1 mM PMSF and 1 mg/mL lysozyme and further incubated for 1 h on ice. The cells were then disrupted by sonication (10 pulses for 30 s each), and the crude lysate obtained was cleared by centrifugation at 80000*g* and 4 °C. The supernatant was mixed with Ni-NTA resin equilibrated with lysis buffer and further incubated with being gently shaken for 1 h at 4 °C. The resin was then loaded on the column, and the flow-through was collected. The column was extensively washed with lysis buffer followed by TN buffer [50 mM Tris-HCl (pH 8.0) and 150 mM NaCl]. The protein was finally eluted with TN buffer containing 250 mM imidazole. The protein was pooled and then desalted using the Biogel P-4 resin pre-equilibrated with TN buffer containing 10% glycerol. The pure protein obtained was then concentrated and stored at −80 °C. The integrity of His-tagged MciZ was examined by Axima-CFR matrix-assisted laser desorption ionization time-of-flight mass spectrometry (Kratos Analytical, Manchester, U.K.). The measured molecular weight matched well with the molecular weight of His-tagged MciZ calculated from the DNA sequence.

The His tag was removed from MciZ using the thrombin clean cleave TM Kit (Sigma) as described in the manufacturer's protocol. Briefly, MciZ (His) was incubated for 12 h at 16 °C with thrombin-agarose in cleavage buffer. Thrombin-agarose was removed from the cleaved protein by centrifugation. The cleavage of the His tag was adjudged by running the samples on 10 to 20% gradient sodium dodecyl sulfate−polyacrylamide gel electrophoresis (SDS−PAGE) and further confirmed by N-terminal protein sequencing.

Fluorescein Isothiocyanate Labeling of MciZ. MciZ (20 μM) was incubated with 60 μM fluorescein isothiocyanate (FITC) at 4 °C for 3 h in 25 mM Pipes buffer. The reaction was quenched by the addition of 5 mM Tris-HCl. Unbound FITC molecules were removed by passing the reaction mixture though a pre-equilibrated gel filtration (Bio-Gel P-4) column.[18] Further, the unbound FITC was removed by continuous cycles of dilution followed by concentration of the labeled protein using a 3 kDa concentrator (Amicon, Millipore). The concentration of MciZ was measured by the Bradford assay,[16] and the concentration of MciZ-bound FITC was determined by using an extinction coefficient of 77000 M^{-1} cm^{-1} at 495 nm. The incorporation stoichiometry of FITC per MciZ was calculated by dividing the MciZ-bound FITC concentration by the protein concentration. The incorporation ratio of FITC in MciZ was found to be 0.3.

Size-Exclusion Chromatography. The interaction between MciZ (without the His tag) and FtsZ was monitored using a size-exclusion column in the presence of 300 mM sodium chloride. The void volume of the Sephadex G-25 (1 cm × 40 cm) column was determined using blue dextran. FtsZ (15 μM) was incubated without or with 10 μM FITC-MciZ (without the His tag) in 25 mM Pipes buffer (pH 6.8) containing 300 mM sodium chloride for 30 min on ice. Proteins were loaded on the pre-equilibrated column and eluted using 25 mM Pipes buffer (pH 6.8) containing 300 mM sodium chloride. The flow rate of the column was adjusted at 0.5 mL/min. The protein concentration of each fraction was determined using the Bradford method,[16] while FITC-MciZ was monitored using the fluorescence intensity at 520 nm. The elution profiles of FITC-MciZ and FtsZ were individually monitored.

As described above, FtsZ (15 μM) was incubated without or with 1 mM GTP in 25 mM Pipes buffer (pH 6.8) containing 300 mM NaCl and 5 mM $MgCl_2$ for 5 min on ice. Then, the reaction mixtures were incubated with 10 μM FITC-MciZ (without the His tag) for 30 min on ice and loaded on a Sephadex G-25 column (1 cm × 40 cm), which was equilibrated with 25 mM Pipes buffer (pH 6.8) containing 300 mM sodium chloride without or with 200 μM GTP. Proteins were eluted using 25 mM Pipes buffer (pH 6.8) containing 300 mM sodium chloride with or without 200 μM GTP.

Determination of the Dissociation Constant of the Interaction of MciZ and FtsZ. FITC-MciZ (1.5 μM) was incubated without and with different concentrations (0.10−6.0 μM) of FtsZ, carbonic anhydrase (2 μM), or lysozyme (2 μM) for 15 min at 25 °C in 25 mM Pipes (pH 6.8). The dissociation constant (K_d) of the interaction between MciZ and FtsZ was determined by fitting the fluorescence data to this quadratic equation[19]

$$\Delta F = \left\{(\Delta F_{max})\left[[P_0] + [L_0] + K_d - \sqrt{([P_0] + [L_0] + K_d)^2 - 4[P_0][L_0]}\right]\right\}/(2[P_0]) \quad (1)$$

where ΔF is the change in the fluorescence intensity of FITC-MciZ in the presence of FtsZ, ΔF_{max} is the change in the fluorescence intensity when MciZ is saturated with FtsZ, and $[P_0]$ and $[L_0]$ are the concentrations of FITC-MciZ and FtsZ, respectively. The change in the fluorescence intensity of each of the reaction set was fit into eq 1 using GraphPad Prism 5 (GraphPad Software). The experiment was performed four times using a fluorescence spectrophotometer (JASCO FP-6500).

Light Scattering Assay. FtsZ (6 μM) was incubated without and with MciZ (5 μM) in 25 mM Pipes buffer (pH 6.8) for 15 min on ice. Then, 5 mM $MgCl_2$, 50 mM KCl, and different concentrations (0, 25, 50, 100, 200, and 500 μM) of GTP were added to the reaction mixtures, and the light scattering signal (500 nm) was monitored at 37 °C for 300 s.[20,21] The experiment was performed three times.

Monitoring the Effect of Nucleotides on the Binding of FtsZ and FITC-MciZ. FtsZ (2 μM) was incubated without and with different concentrations of GTP (1, 2, 5, 10, 20, 30, 50, 100, and 200 μM), GDP (10, 20, 30, 50, 100, and 200 μM), or ATP (100 and 500 μM) in 25 mM Pipes buffer (pH 6.8), 50 mM KCl, and 5 mM $MgCl_2$ for 5 min on ice. FITC-MciZ (1.5 μM) was added to the reaction mixture and the mixture incubated for an additional 10 min at 25 °C. The emission spectra were recorded in the range of 510−600 nm using 495 nm as the excitation wavelength. The change in the fluorescence intensity was plotted in the presence of different concentrations of nucleotides.

The fluorescence intensity of FITC-MciZ in the presence of a fixed concentration of FtsZ was found to decrease with an increasing concentration of GTP. The apparent dissociation constant (K_i) of the interaction between GTP and FtsZ was calculated by the fitting the fluorescence data to eq 2

$$K_i = EC_{50}/(1 + [L]/K_d) \quad (2)$$

where K_i is the concentration of GTP that binds to half the binding sites on FtsZ, [L] is the concentration of MciZ, K_d is the dissociation constant of MciZ and FtsZ, and EC_{50} (half-maximal effective concentration) refers to the concentration of an inhibitor that causes inhibition of fluorescence halfway between the minimum and maximum.[22] The data were analyzed using GraphPad Prism.[23] The experiment was performed three times.

Effect of MciZ on Binding of 2′,3′-*O*-(2,4,6-Trinitrocyclohexadienylidene)-GTP (TNP-GTP) to FtsZ. FtsZ (6 μM) was incubated in 25 mM Pipes buffer (pH 6.8) containing 5 mM $MgCl_2$, 10% glycerol, and 200 mM NaCl without and with 5 and 10 μM MciZ for 15 min on ice. TNP-GTP (15 μM) was added to the reaction mixtures, and the mixtures were incubated on ice for 2 h. The emission spectra were recorded in the range of 500−600 nm using 410 nm as the excitation wavelength. Appropriate blank spectra were taken and subtracted from the respective spectra.[24]

The interaction between TNP-GTP and FtsZ in the absence and presence of MciZ (without the His tag) was also monitored by size-exclusion chromatography using a Sephadex G-25 column (1 cm × 6.7 cm). FtsZ (10 μM) was first incubated without or with 10 μM MciZ (without the His tag) in 25 mM Pipes buffer (pH 6.8) containing 200 mM NaCl and 5 mM $MgCl_2$ for 15 min on ice. Then, TNP-GTP (15 μM) was added to the reaction mixtures, and the mixtures were incubated for an additional 2 h on ice. Reaction mixtures (200 μL) were loaded on the pre-equilibrated column and eluted using 25 mM Pipes buffer (pH 6.8) containing 200 mM sodium chloride. The flow rate of the column was adjusted to 0.3 mL/min. The amount of protein in each fraction was determined by the Bradford method, while the fluorescence intensity of TNP-GTP was monitored at 540 nm using 410 nm as the excitation wavelength. FtsZ (10 μM) and only TNP-GTP (15 μM) in the absence of FtsZ were also eluted separately using the same column.

Interaction of MciZ with the C-Terminal Tail of FtsZ. CTP17, a C-terminal tail (residues 366−382) peptide of FtsZ having a DDTLDIPTFLRNRNKRG amino acid sequence,[12] was used to examine whether the C-terminal tail of FtsZ is involved in the binding interaction of FtsZ and MciZ. MciZ (10 μM) was incubated without or with CTP17 peptide (50 μM) in 25 mM Pipes buffer (pH 6.8) for 30 min on ice. FtsZ (6 μM) was added to the reaction mixture and the mixture incubated for an additional 30 min on ice. Then 5 mM $MgCl_2$, 50 mM KCl, and 200 μM GTP were added, and the light scattering signal (at 500 nm) was monitored at 37 °C for 600 s. Respective control readings were taken for each of the reaction sets.

Effects of MciZ, M19I, and R21P on the GTPase Activity of FtsZ. The purity of peptides MKVHRMPKGVV-LVGKAWEI (M19I) and RAKLKEYGRTFQYVKDWISKP (R21P) was checked using HPLC, and the molecular weight was determined by electrospray ionization mass spectrometry. The purities of M19I and R21P were found to be >95 and >85%, respectively.

FtsZ (6 μM) was incubated without and with different concentrations of MciZ (without the His tag), M19I, or R21P in 25 mM Pipes buffer (pH 6.8) containing 5 mM $MgCl_2$ and 250 mM KCl for 15 min on ice. Then, 500 μM GTP was added to the reaction mixtures and incubated at 37 °C. The amount of inorganic phosphate released was measured after hydrolysis for 10 min using the standard malachite green assay.[24,25]

Sedimentation Assay. FtsZ (6 μM) was polymerized without and with either 10 μM MciZ (without the His tag), 20 M19I, 40 μM M19I, or 40 μM R21P in 25 mM Pipes buffer (pH 6.8) containing 5 mM $MgCl_2$, 250 mM KCl, and 200 μM GTP for 5 min. The polymers were collected by high-speed centrifugation at 280000*g* for 30 min at 30 °C and analyzed by Coomassie blue staining of the SDS−PAGE gel.

Electron Microscopic Study. FtsZ (5 μM) was incubated without and with either 10 μM MciZ (without the His tag), 20 μM M19I, 40 μM M19I, or 40 μM R21P in 25 mM Pipes buffer (pH 6.8) containing 5 mM $MgCl_2$ and 250 mM KCl for 15 min on ice. Then, 200 μM GTP was added to the reaction mixtures and polymerized at 37 °C for 10 min. Polymeric suspensions were transferred onto Formvar carbon-coated copper grids (300 meshes) and negatively stained with a 2% uranyl acetate solution.[21,26] The samples were examined using a transmission electron microscope (FEI Tecnai G^2 12).

Immunofluorescence Microscopy. *E. coli* BL21 cells containing the mciz plasmid were grown at 37 °C in LB medium. The cells were induced (OD_{600} = 0.6) with 1 mM IPTG for 2 h. Cells were fixed using 2.5% formaldehyde and 0.04% glutaraldehyde. FtsZ was stained with the polyclonal FtsZ antibody raised in rabbit followed by the Cy3-conjugated goat anti-rabbit secondary antibody.[26] Nucleoids were stained using 20 μg/mL DAPI. The cells were mounted on a glass slide and visualized under a fluorescence microscope.

RESULTS

MciZ Inhibits the Assembly and GTPase Activity of FtsZ. As reported previously,[14] MciZ and MciZ (His) were found to inhibit the assembly of FtsZ in similar manner (Figure S1A of the Supporting Information). For example, the assembly of FtsZ was inhibited by 90 ± 3 and 88 ± 7% in the presence of 10 μM MciZ and MciZ (His), respectively. Further, FITC-MciZ was also found to inhibit the assembly of FtsZ (Figure S1B of the Supporting Information). For example, the light scattering signal of FtsZ assembly was reduced by 33, 57, and 78% in the presence of 5, 7, and 10 μM FITC-MciZ, respectively, suggesting that the covalently modified MciZ retains its ability to inhibit FtsZ assembly. In addition, the level of assembly of FtsZ was also found to be reduced by 35, 55, and 72% in the presence of 5, 7, and 10 μM FITC-MciZ(his), respectively, indicating that the His tag does not influence the

polymerization inhibitory activity of FITC-MciZ (data not shown).

Consistent with the previous study,[14] the GTPase activity of FtsZ was reduced by 22 ± 4, 38 ± 8, 54 ± 5, and 59 ± 3% in the presence of 1.5, 3, 5, and 10 μM MciZ, respectively (Figure S2 of the Supporting Information). The GTPase activity of FtsZ was also found to be reduced by 26 ± 4, 44 ± 3, and 50 ± 4% in the presence of 3, 5, and 10 μM MciZ (His), respectively. The results together showed that MciZ and MciZ (His) exerted similar effects on the assembly and GTPase activity of FtsZ.

MciZ Binds to FtsZ in Vitro. The interaction between FITC-MciZ and FtsZ was examined by size-exclusion chromatography in the presence of 300 mM sodium chloride (Figure 1). When loaded separately, FITC-MciZ and FtsZ were found to be eluted at volumes of 61 and 27 mL, respectively. The mixture of FITC-MciZ and FtsZ was loaded on the same column, and the elution profile of the mixture showed FITC-MciZ fluorescence at two distinct fractions, namely, at elution volumes of 26.5 and 61 mL. The peak at 61 mL corresponded to FITC-MciZ, while the peak at 26.5 mL indicated the formation of the FtsZ−MciZ complex. Because the molecular weight of FITC-MciZ is low, therefore, not much difference in the elution volume of the complex (26.5 mL) and FtsZ (27 mL) was observed during gel filtration. The result indicated that MciZ binds to FtsZ in vitro. FITC-MciZ (His) was also found to co-elute with FtsZ in a similar fashion (data not shown).

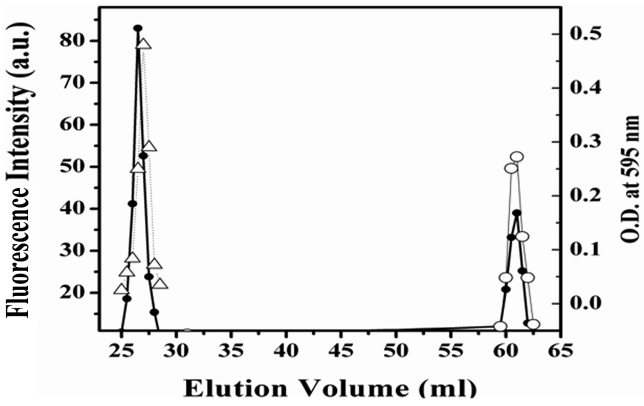

Figure 1. FtsZ directly interacted with MciZ in vitro. The binding of FITC-MciZ (without the His tag) to FtsZ was monitored using size-exclusion chromatography in the presence of 300 mM NaCl. The elution profiles of FtsZ (△), FITC-MciZ (○), and FITC-MciZ in the presence of FtsZ (●) are shown. FITC-MciZ was monitored by measuring the fluorescence intensity at 520 nm, while FtsZ was monitored by measuring the absorbance at 595 nm using Bradford reagent.

The fluorescence intensity of FITC-MciZ was found to increase in a concentration-dependent manner in the presence of an increasing concentration of FtsZ (Figure 2A). For example, the fluorescence intensity of FITC-MciZ was increased by 38 ± 7 and 57 ± 7% in the presence of 1 and 3 μM FtsZ, respectively. The fluorescence intensity of FITC-MciZ could increase upon its binding to FtsZ for several possible reasons. The increase in the fluorescence intensity may be due to the immobilization of FITC-MciZ upon its binding to FtsZ, which is ∼10 times larger than MciZ. In support of this, the fluorescence polarization of free FITC-MciZ was found to increase from 0.03 ± 0.002 to 0.13 ± 0.006 in the presence of 6 μM FtsZ. Alternatively, the fluorescence intensity of FITC-MciZ may increase upon binding to FtsZ because of the protection from the solvent quenching and/or the quenching effect of the nearby residues of FITC-MciZ may weaken because of a conformational change in the protein. In contrast, 2 μM carbonic anhydrase and lysozyme did not change the fluorescence intensity of FITC-MciZ, indicating that the enhancement of the fluorescence intensity of FITC-MciZ in the presence of FtsZ was not due to a nonspecific protein−protein interaction (Figure 2B). The dissociation constant (K_d) of the interaction between MciZ and FtsZ was determined to be 0.3 ± 0.1 μM, indicating a strong interaction between these proteins (Figure 2A, inset).

Several regulators of FtsZ are reported to bind to the C-terminal tail of FtsZ.[2,12,27,28] We have used a FtsZ construct (FtsZΔC16) lacking 16 C-terminal residues[12] to examine whether MciZ interacts with FtsZ through its C-terminal tail. Similar to the binding reaction with full-length FtsZ, the fluorescence intensity of FITC-MciZ was found to increase in the presence of FtsZΔC16 in a concentration-dependent manner (Figure S3A of the Supporting Information). A K_d of

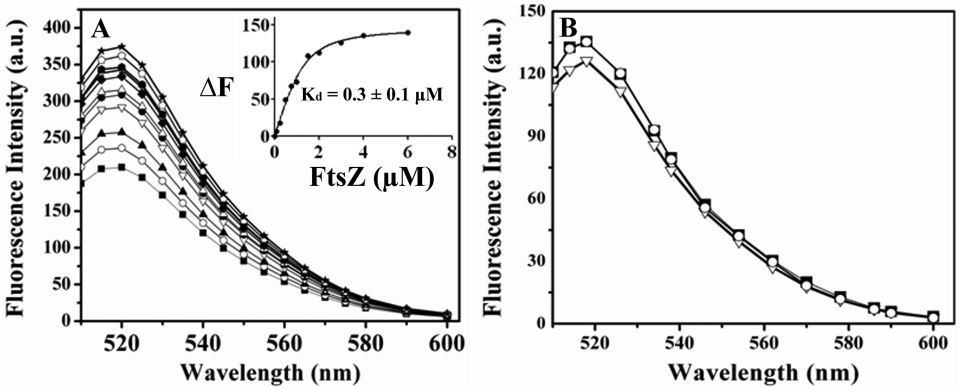

Figure 2. Determination of the dissociation constant of the interaction of MciZ and FtsZ. (A) FtsZ increased the fluorescence intensity of FITC-MciZ. The fluorescence intensity of 1.5 μM FITC-MciZ was monitored in the absence (■) and presence of (○) 0.1, (▲) 0.25, (▽) 0.50, (●) 0.75, (△) 1, (◆) 1.5, (□) 2, (⬢) 3, (⬠) 5, and (★) 6 μM FtsZ. The inset shows the change in fluorescence intensity of FITC-MciZ at 520 nm with the increasing concentration of FtsZ. The reported K_d value is an average of four experiments, and the standard deviation is given. (B) FITC-MciZ (1.5 μM) was incubated in the absence (▽) and presence of 2 μM (○) lysozyme or (■) carbonic anhydrase. The fluorescence spectra were measured using 495 nm as the excitation wavelength.

dx.doi.org/10.1021/bi301237m | *Biochemistry* 2013, 52, 392−401

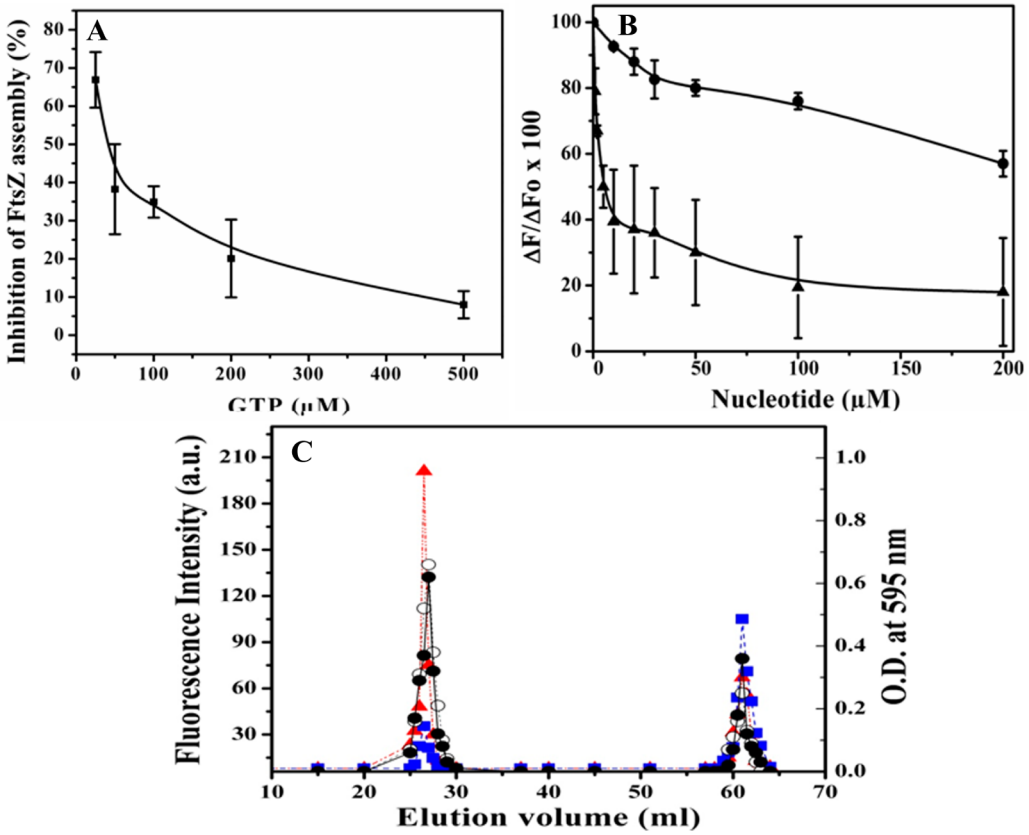

Figure 3. GTP weakened the interaction between MciZ and FtsZ. (A) GTP reduced the inhibitory effect of MciZ (5 μM) on the assembly of 6 μM FtsZ. (B) Both GTP and GDP weakened the binding of MciZ to FtsZ. FtsZ (2 μM) was incubated without and with different concentrations of either GTP or GDP on ice for 5 min. Then, FITC-MciZ (1.5 μM) was added to the reaction milieu, and the fluorescence spectra were recorded. ΔF_0 and ΔF represent the change in the fluorescence intensity of FITC-MciZ at 520 nm in the presence of FtsZ without and with either GTP (▲) or GDP (●). (C) GTP inhibited the binding of FITC-MciZ to FtsZ. FtsZ (15 μM) was first incubated without or with 1 mM GTP for 5 min on ice, and the mixtures were then incubated with 10 μM FITC-MciZ (without the His tag) for 30 min on ice. The protein mixtures were loaded on the column and eluted as described in Experimental Procedures. FITC-MciZ was monitored by measuring the fluorescence intensity at 520 nm, and the protein concentration was monitored by adding Bradford reagent and measuring the OD at 595 nm. The fluorescence intensity at 520 nm in the absence (red triangles) and presence (blue squares) of 1 mM GTP and the absorbance at 595 nm in the absence (○) and presence (●) of 1 mM GTP are shown.

0.5 ± 0.1 μM was estimated for the binding interaction of MciZ and FtsZΔC16 (inset of Figure S3A of the Supporting Information). The result suggested that the C-terminal tail of FtsZ is not required for the binding of FtsZ to MciZ. In addition, a 17-mer C-terminal (residues 366−382) FtsZ peptide having a DDTLDIPTFLRNRNKRG (CTP17) amino acid sequence[12] was used to probe whether MciZ binds to the C-terminus of FtsZ. We thought that if MciZ binds to the C-terminal tail of FtsZ, then CTP17 should nullify the inhibitory effect of MciZ on the assembly of FtsZ. CTP17 had no influence on the inhibitory effect of MciZ on the FtsZ assembly (Figure S3B of the Supporting Information). For example, 10 μM MciZ inhibited the light scattering intensity of the assembly of FtsZ by 63 and 60% in the absence and presence of 50 μM CTP17, respectively, suggesting that MciZ does not interact with the C-terminal tail of FtsZ

GTP Reduces the Inhibitory Effect of MciZ on FtsZ Polymerization. Consistent with the previous observation,[14] the inhibitory effect of MciZ on the assembly of FtsZ was found to weaken with an increasing concentration of GTP (Figure 3A). In the presence of 25, 50, 100, 200, and 500 μM GTP, the level of inhibition of FtsZ assembly by MciZ was found to be 67 ± 7.3, 38.3 ± 11.8, 35 ± 4, 20 ± 10, and 8 ± 3.6%, respectively, with respect to the control (in the absence of MciZ with an equal concentration of GTP).

We thought that GTP might reduce the inhibitory effect of MciZ on FtsZ polymerization by two ways. (i) MciZ itself hydrolyzes GTP and thereby depletes the available GTP pool, and (ii) GTP weakens the binding of MciZ and FtsZ in a concentration-dependent manner. To distinguish between these two possibilities, we first determined whether MciZ displays GTPase activity. MciZ did not hydrolyze GTP. We then determined if GTP affects the binding of FtsZ and MciZ (Figure 3B). For this, we monitored the change in the fluorescence intensity of FITC-MciZ upon interaction with FtsZ in the absence and presence of GTP. The fluorescence intensity of FITC-MciZ increased when it was incubated with FtsZ, indicating the interaction between FtsZ and MciZ (Figure 2A). The increase in the fluorescence intensity of FITC-MciZ in the presence of a fixed concentration of FtsZ decreased with an increasing concentration of GTP (Figure 3B). For example, 10 and 200 μM GTP decreased the fluorescence enhancement by 61 ± 19 and 82 ± 20%, respectively. The result suggested that GTP inhibited the interaction between FtsZ and MciZ. The apparent dissociation constant for the binding of GTP to FtsZ was estimated to be 1.2 ± 0.3 μM (Figure S4A of the

dx.doi.org/10.1021/bi301237m | *Biochemistry* 2013, 52, 392−401

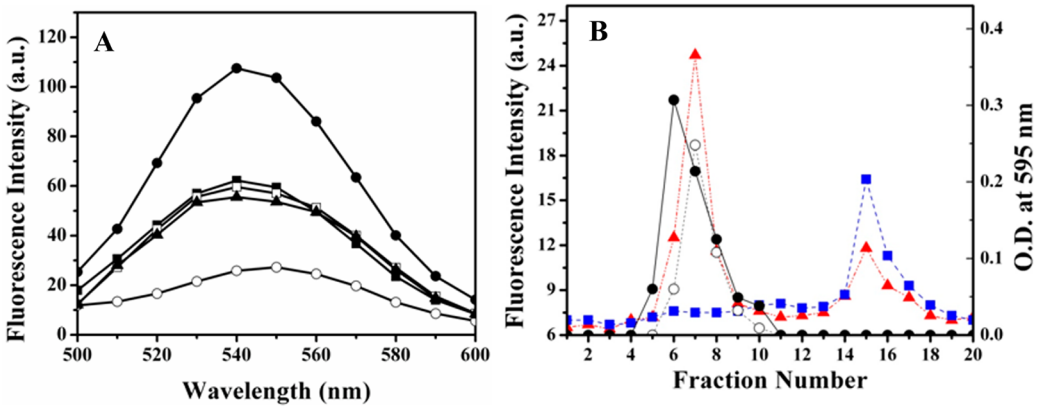

Figure 4. MciZ weakened the binding of TNP-GTP to FtsZ. FtsZ (6 μM) was incubated with TNP-GTP (15 μM) in the absence (●) and presence of 5 (□) and 10 μM MciZ (▲) for 2 h on ice. GTP (20 μM) was used as a positive control (■). The spectrum of 15 μM TNP-GTP (○) in the absence of FtsZ was also recorded. The emission spectra were recorded using 410 nm as the excitation wavelength. (B) MciZ weakened the interaction between FtsZ and TNP-GTP. The elution profile was monitored by measuring the fluorescence intensity at 540 nm and also by measuring the absorbance at 595 nm using Bradford reagent. The fluorescence intensity of TNP-GTP was plotted in the absence (red triangles) and presence (blue squares) of MciZ. The elution of proteins was monitored by measuring absorbance at 595 nm in the absence (○) and presence (●) of MciZ.

Supporting Information), which was consistent with the reported value of 3.7 μM.[29] Further, GDP also weakened the binding of MciZ to FtsZ, albeit to a lesser extent than GTP (Figure 3B). For example, the binding was found to be inhibited by 7 ± 1 and 42 ± 4% in the presence of 10 and 200 μM GDP, respectively (Figure 3B). The apparent dissociation constant for the binding of GDP to FtsZ was calculated to be 13.2 ± 2 μM (Figure S4B of the Supporting Information). However, ATP (100 and 500 μM) had no effect on the fluorescence intensity of FITC-MciZ in the presence of FtsZ, suggesting that ATP did not detectably inhibit the binding of MciZ to FtsZ. The results indicate that the inhibition of the MciZ−FtsZ interaction is specific to guanosine nucleotides.

The effect of GTP on the binding interaction of MciZ with FtsZ was further investigated by size-exclusion chromatography. As observed in Figure 1, FITC-MciZ was eluted in the void volume (26.5 mL) in the presence of FtsZ, suggesting that FITC-MciZ formed a complex with FtsZ. The fluorescence intensity of FITC-MciZ in the void volume (26.5 mL) strongly decreased in the presence of GTP, suggesting that GTP inhibited the binding of FITC-MciZ to FtsZ (Figure 3C).

GTP inhibited the binding of MciZ with FtsZ; therefore, we probed if MciZ could influence the binding of GTP to FtsZ. TNP-GTP, a fluorescent analogue of GTP, has been reported to bind to the GTP site on FtsZ.[24,30] In accordance with previous reports,[24,30] GTP reduced the fluorescence intensity of the TNP-GTP−FtsZ complex by 64 ± 7% with respect to the control, indicating that they compete for the same site on FtsZ (Figure 4A). We further found that 5 and 10 μM MciZ reduced the fluorescence of the TNP-GTP−FtsZ complex by 69 ± 8 and 72 ± 6%, respectively, indicating that MciZ inhibits the binding of TNP-GTP to FtsZ (Figure 4A). The result indicated that MciZ and GTP compete with each other for their binding to FtsZ, and thus, they may share a common binding site on FtsZ.

To further examine whether MciZ inhibits binding of TNP-GTP to FtsZ, we monitored the binding of TNP-GTP to FtsZ using a size-exclusion column (Figure 4B). FtsZ and free TNP-GTP in the absence of FtsZ were found to be eluted with peaks having fraction numbers 7 and 15, respectively (data not shown). When a mixture containing FtsZ and TNP-GTP was loaded on the column, TNP-GTP was eluted at two different peaks (Figure 4B). The peak at fraction 7 indicated the formation of the FtsZ−TNP-GTP complex, while the peak at fraction number 15 corresponded to free TNP-GTP (Figure 4B). The fluorescence intensity of TNP-GTP at fraction number 7 was found to decrease substantially when FtsZ was preincubated with MciZ, indicating that MciZ competes with TNP-GTP for its binding to FtsZ.

To further examine the role of GTP hydrolysis in the MciZ-mediated inhibition of FtsZ assembly, we used guanosine-5′-[(β,γ)-methyleno]triphosphate (GMPPCP), a nonhydrolyzable analogue of GTP. MciZ inhibited the assembly of FtsZ in the presence of 200 μM GMPPCP, indicating that the inhibition of FtsZ assembly by MciZ does not occur through the perturbation of the GTP hydrolysis step. For example, the level of assembly of FtsZ was reduced by 23 and 81% in the presence of 5 and 10 μM MciZ, respectively (Figure S5 of the Supporting Information).

Overexpression of MciZ Inhibits Z-Ring Formation in *E. coli* Cells. The GTP binding site on FtsZ and the proximate residues are almost conserved in many species of bacteria,[31−33] and the results of this study indicated that MciZ shares its binding site on FtsZ with GTP. Therefore, it is logical to assume that MciZ might be able to bind to other bacterial FtsZs and inhibit their polymerization. To assess this, we first examined the interaction between purified MciZ and *E. coli* FtsZ in vitro. FITC-MciZ was incubated with different concentrations of *E. coli* FtsZ. The fluorescence intensity of MciZ increased in the presence of *E. coli* FtsZ in a concentration-dependent manner. For example, the fluorescence intensity of FITC-MciZ was increased by 26 and 31% in the presence of 1.5 and 3 μM *E. coli* FtsZ, respectively, suggesting that MciZ interacts with *E. coli* FtsZ (Figure S6A of the Supporting Information). Further, MciZ inhibited the assembly of purified *E. coli* FtsZ. For example, in the presence of MciZ (10 μM), the magnitude of the light scattering signal was reduced by 81% as compared to that of the control (Figure S6B of the Supporting Information).

Because MciZ bound to *E. coli* FtsZ and inhibited its assembly, we examined whether MciZ could inhibit the formation of the Z-ring in *E. coli* cells. MciZ was expressed

dx.doi.org/10.1021/bi301237m | *Biochemistry* 2013, 52, 392−401

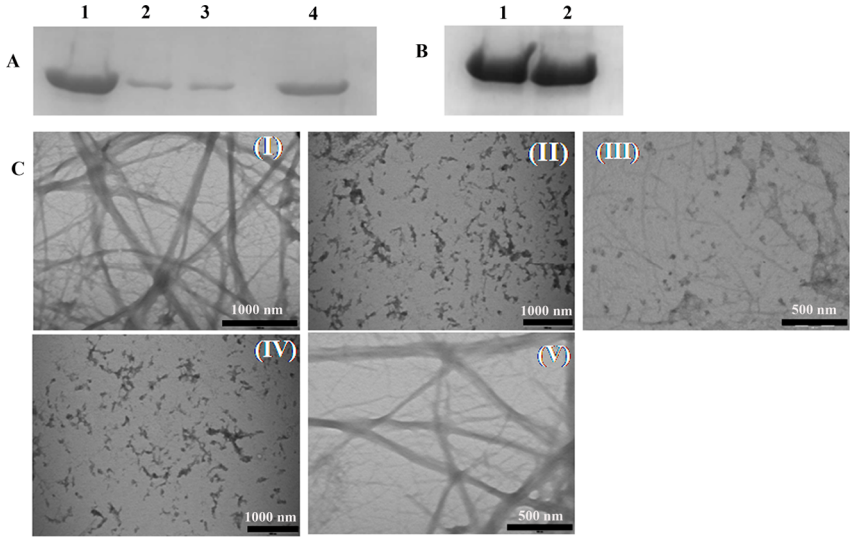

Figure 5. M19I inhibited the assembly of FtsZ. (A) MciZ and M19I reduced the polymerized amount of FtsZ. FtsZ (6 μM) was polymerized without and with either 10 μM MciZ (without the His tag) or 20 and 40 μM M19I in the presence of 250 mM KCl as described in Experimental Procedures. FtsZ polymers were collected by centrifugation and analyzed by Coomassie blue staining of the SDS−PAGE gel. Lanes 1−4 represent the polymerized amount of FtsZ alone or in the presence of 10 μM MciZ, 40 μM M19I, and 20 μM M19I, respectively. (B) Lanes 1 and 2 represent the polymerized amount of FtsZ in the absence and presence of 40 μM R21P, respectively. (C) FtsZ (5 μM) was polymerized without (I) and with 10 μM MciZ (without the His tag) (II), 20 (III) and 40 μM M19I (IV), or 40 μM R21P (V) in the presence of 250 mM KCl as described in Experimental Procedures.

from plasmid pAH124 (PT7-His6-MciZ *kan*). Under the conditions used, IPTG treatment alone had no visible effect on Z-ring formation in BL21 cells (without the MciZ plasmid). BL21 cells transformed with MciZ plasmid were grown in the absence and presence of 1 mM IPTG for 2 h. While most of the control cells were found to contain two nucleoids, the cells expressing MciZ were found be elongated and contained two, four, eight, or more nucleoids. Further, the expression of MciZ did not appear to affect the nucleoid segregation in *E. coli* cells, indicating that MciZ inhibited FtsZ assembly in the Z-ring and blocked cytokinesis in these cells (Figure S6C of the Supporting Information). The results suggested that MciZ can inhibit FtsZ assembly and Z-ring formation.

The M19I Peptide Inhibits the Assembly and GTPase Activity of FtsZ in Vitro. I19L, a stathmin-derived peptide, was found to inhibit the assembly and bundling of FtsZ.[34] An analysis of the sequences of I19L and MciZ suggested that the sequence of I19L is 32.5 and 64% similar with that of the full-length and N-terminal (M19I) parts of MciZ, respectively, indicating that the N-terminal part of MciZ might be responsible for its interaction with FtsZ. To verify this idea, we constructed M19I (a peptide containing 19 residues from the N-terminal part of MciZ) and R21P (a peptide containing 21 residues from the C-terminal part of MciZ) peptides.

MciZ (10 μM) inhibited the amount of polymerized FtsZ by 65.4 ± 13.6%, while 20 and 40 μM M19I inhibited FtsZ polymerization by 22 ± 9.2 and 64 ± 18.4%, respectively (Figure 5A). However, R21P had no effect on the assembly of FtsZ (Figure 5B). The effects of MciZ, M19I, and R21P on the assembly of FtsZ were also examined by electron microscopy (Figure 5C). MciZ visibly slowed the filamentous assembly of FtsZ (Figure 5C). Similar to the inhibitory effects of MciZ on the assembly of FtsZ, M19I (20 μM) also clearly reduced the number of FtsZ filaments per field of view. M19I (40 μM) strongly inhibited the filamentous assembly of FtsZ and also caused aggregation of FtsZ (Figure 5C). R21P did not have any visible inhibitory effect on the assembly of FtsZ (Figure 5C). These results together suggested that M19I inhibits the assembly of FtsZ while R21P does not affect the assembly of FtsZ.

As shown previously,[14] MciZ inhibited the GTPase activity of FtsZ (Figure S2 of the Supporting Information); therefore, we examined whether M19I and R21P could inhibit the GTPase activity of FtsZ (Figure 6). Like MciZ, the M19I peptide also

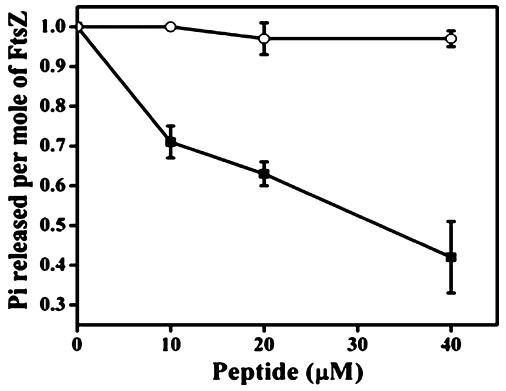

Figure 6. M19I suppressed the GTPase activity of FtsZ. FtsZ (6 μM) was polymerized in the absence or presence of different concentrations of either M19I (■) or R21P (□). The rate of GTP hydrolysis of FtsZ in the absence of the peptides was estimated to be 1 mol of P_i per mole of FtsZ per minute.

inhibited the GTPase activity of FtsZ in a concentration-dependent manner; for example, 20 and 40 μM M19I reduced the GTPase activity by 42 and 55%, respectively. The partial inhibition of the GTPase activity may be due to the formation of FtsZ oligomers, which are capable of hydrolyzing GTP. However, R21P did not show any detectable effect on the GTPase activity of FtsZ (Figure 6).

dx.doi.org/10.1021/bi301237m | *Biochemistry* 2013, 52, 392−401

DISCUSSION

The assembly of FtsZ to form a Z-ring at the midcell is of prime importance in bacterial cell division. The timing and positioning of the Z-ring are tightly regulated by a number of accessory proteins.[2,4,35] MciZ, a recently identified FtsZ assembly inhibitor, is suggested to prevent Z-ring formation during sporulation in *B. subtilis*.[14] In this study, we provide evidence suggesting that GTP plays an important role in regulating the interaction of MciZ and FtsZ. MciZ was found to bind to FtsZ with a K_d of 0.3 ± 0.1 μM, suggesting that it binds to FtsZ in vitro with a high affinity. The results indicate that unlike several other regulators of FtsZ assembly such as EzrA, SepF, and FtsA, MciZ does not bind to the C-terminal tail of FtsZ.[2,12,27,28] Therefore, MciZ does not appear to compete with other regulators of FtsZ assembly for its binding to FtsZ. The finding partly explains why MciZ is expressed only during sporulation. Further, M19I, a 19-residue peptide of MciZ, having the same sequence as the N-terminal part of MciZ, was found to mimic the polymerization inhibitory activity of MciZ in vitro, while R21P (a C-terminal 21-residue peptide of MciZ) had no effect on the assembly of FtsZ.

As reported previously,[14] MciZ was found to efficiently inhibit the assembly of FtsZ in the presence of low and moderate concentrations of GTP, while it had a less inhibitory effect on the assembly of FtsZ in the presence of high concentrations of GTP (Figure 3A). The decrease in the inhibitory effect of MciZ in the presence of high concentrations of GTP may be due to two possible reasons. One of the possibilities is that MciZ inhibits FtsZ assembly by hydrolyzing the available GTP when the assembly milieu contains low concentrations of GTP, whereas it could not inhibit FtsZ assembly in the presence of high concentrations of GTP because it could not completely exhaust the available GTP. This possibility can be ruled out because MciZ does not have the ability to hydrolyze GTP and MciZ also inhibits the assembly of FtsZ in the presence of GMPPCP, a non-hydrolyzable analogue of GTP, suggesting that hydrolysis of GTP may not be critical for MciZ-mediated inhibition of FtsZ assembly. The second possibility is that GTP inhibits the binding of MciZ to FtsZ. In support of this, MciZ was found to inhibit the binding of TNP-GTP, a GTP analogue, to FtsZ. Further, both GTP and GDP inhibited the binding of MciZ to FtsZ. The results together suggested that MciZ and GTP seem to have overlapping binding sites on FtsZ and provided an explanation for the influence of GTP on the polymerization inhibitory ability of MciZ. However, it is difficult to completely rule out the possibility that the binding of MciZ to FtsZ allosterically modifies the binding site of GTP on FtsZ, which weakens the binding of GTP to FtsZ.

It has been suggested that when GTP interacts with FtsZ, the T7 loop of FtsZ protrudes from the FtsZ monomer and binds to another GTP-bound FtsZ monomer.[36,37] The binding of GTP to FtsZ is known to induce a conformational change in FtsZ.[38,39] Though both GTP and GDP inhibited the interaction of MciZ and FtsZ, the effect was significantly higher in the presence of GTP than in the presence of GDP, which may be due to the lower binding affinity of GDP for FtsZ as compared to the binding affinity of GTP for FtsZ.

We thought that if MciZ has a binding site at or near the GTP binding pocket of FtsZ then it might interact with *E. coli* FtsZ because the GTP binding motif of *E. coli* FtsZ is similar to that of *B. subtilis* FtsZ.[31−33] The sequence comparison of the predicted binding region of MciZ in *B. subtilis* 168 and *E. coli* K12 substr.W3110 showed 97.4% sequence similarity (Figure S6D of the Supporting Information). As anticipated, MciZ was found to bind to *E. coli* FtsZ and to inhibit the assembly of *E. coli* FtsZ in vitro. Moreover, the expression of MciZ in *E. coli* cells caused perturbation of the Z-ring and also inhibited cytokinesis in *E. coli* cells. The findings further favor the argument that GTP and MciZ share their binding sites on FtsZ.

The binding site of GTP on FtsZ is highly conserved in several bacterial species.[31−33] Small molecules or peptide-derived inhibitors that target the GTP binding site are found to inhibit FtsZ assembly.[40] For example, several C8-substituted GTP analogues such as chloro-, bromo-, iodo-, and methoxy-GTP are shown to inhibit the assembly of FtsZ by competing with GTP.[41] MciZ is found to be expressed during the sporulation of *B. subtilis* cells,[14] and the intracellular level of GTP decreases during sporulation.[42] MciZ efficiently inhibited the assembly of FtsZ in the presence of low concentrations of GTP, and the results of this study indicate that MciZ and GTP compete for the same binding site on FtsZ. Therefore, it is logical to suggest that MciZ inhibits the assembly of FtsZ when the intracellular concentration of GTP is low and thereby blocks bacterial cell division.

In conclusion, we have shown that GTP plays an important role in the interaction of MciZ with FtsZ, and the results provide evidence in support of a mechanism by which FtsZ assembly is regulated during sporulation in *B. subtilis* cells. The identification of an active part of MciZ that inhibits FtsZ assembly might help in the design of peptide inhibitors of FtsZ assembly.

ASSOCIATED CONTENT

Supporting Information

Effects of MciZ and MciZ (His) on the kinetics of FtsZ assembly (Figure S1A), effects of FITC-MciZ on the kinetics of FtsZ assembly (Figure S1B), inhibition of GTPase activity of FtsZ by MciZ (Figure S2), the absence of interaction of MciZ with the C-terminal tail of FtsZ (Figure S3), GTP and GDP reducing the level of binding of FITC-MciZ to FtsZ (the graphs were used to determine the apparent dissociation constants for the binding of GTP and GDT to FtsZ) (Figure S4), inhibition of the assembly of FtsZ by MciZ in the presence of GMPPCP (Figure S5), interaction of MciZ with *E. coli* FtsZ and inhibition of its polymerization (Figure S6A,B), heterologous expression of MciZ in *E. coli* cells that causes cell elongation (Figure S6C), and sequence similarity of the GTP binding site and its proximate residues in FtsZ from *B. subtilis* 168 and *E. coli* K12 substr.W3110 (Figure S6D). This material is available free of charge via the Internet at http://pubs.acs.org.

AUTHOR INFORMATION

Corresponding Author

*Indian Institute of Technology Bombay, Mumbai 400076, India. Phone: +91-22-25767838. Fax: +91-22-25723480. E-mail: panda@iitb.ac.in.

Funding

The work is supported by a grant (to D.P.) from Department of Science and Technology, Government of India, and by a Ramalingaswamy fellowship (to A.K.) from Department of Biotechnology, Government of India. S.R. is supported by a fellowship from the Indian council of Medical Research.

Notes

The authors declare no competing financial interest.

■ ACKNOWLEDGMENTS

We sincerely thank Dr. Richard Losick (Harvard University, Cambridge, MA) for providing us the MciZ clone. We thank the Center for Research in Nanotechnology and Science, Indian Institute of Technology Bombay, for providing the transmission electron microscopy facility. We thank Sonia Kapoor, Jayant Asthana, Ankit Rai, and Bhavya Jindal for critical reading of the manuscript.

■ ABBREVIATIONS

FITC, fluorescein isothiocyanate; TNP-GTP, 2′,3′-*O*-(2,4,6-trinitrocyclohexadienylidene)-GTP; SD, standard deviation; GMPPCP, guanosine-5′-[(β,γ)-methyleno]triphosphate; IPTG, isopropyl β-D-1-thiogalactopyranoside

■ REFERENCES

(1) Margolin, W. (2000) FtsZ and the division of prokaryotic cells and organelles. *Nat. Rev. Mol. Cell Biol. 56*, 862−871.

(2) Adams, D. W., and Errington, J. (2009) Bacterial cell division: Assembly, maintenance and disassembly of the Z ring. *Nat. Rev. Microbiol. 7*, 642−653.

(3) Kapoor, S., and Panda, D. (2009) Targeting FtsZ for antibacterial therapy: A promising avenue. *Expert Opin. Ther. Targets 13*, 1037−1051.

(4) Erickson, H. P., Anderson, D. E., and Osawa, M. (2010) FtsZ in bacterial cytokinesis: Cytoskeleton and force generator all in one. *Microbiol. Mol. Biol. Rev. 74*, 504−528.

(5) Stricker, J., Maddox, P., Salmon, E. D., and Erickson, H. P. (2002) Rapid assembly dynamics of the *Escherichia coli* FtsZ-ring demonstrated by fluorescence recovery after photo bleaching. *Proc. Natl. Acad. Sci. U.S.A. 99*, 3171−3175.

(6) Anderson, D. E., Gueiros-Filho, F. J., and Erickson, H. P. (2004) Assembly dynamics of FtsZ rings in *Bacillus subtilis* and *Escherichia coli* and effects of FtsZ-regulating proteins. *J. Bacteriol. 186*, 5775−5778.

(7) Dai, K., Mukherjee, A., Xu, Y., and Lutkenhaus, J. (1994) Mutations in *ftsz* that confer resistance to SulA affect the interaction of FtsZ with GTP. *J. Bacteriol. 176*, 130−136.

(8) Beuria, T. K., Singh, P., Surolia, A., and Panda, D. (2009) Promoting assembly and bundling of FtsZ as a strategy to inhibit bacterial cell division: A new approach for developing novel antibacterial drugs. *Biochem. J. 423*, 61−69.

(9) Jaiswal, R., Patel, R. Y., Asthana, J., Jindal, B., Balaji, P. V., and Panda, D. (2010) E93R substitution of *Escherichia coli* FtsZ induces bundling of protofilaments, reduces GTPase activity, and impairs bacterial cytokinesis. *J. Biol. Chem. 285*, 31796−31805.

(10) Singh, P., and Panda, D. (2010) FtsZ inhibition: A promising approach for antistaphylococcal therapy. *Drug News Perspect. 23*, 295−304.

(11) Singh, J. K., Makde, R. D., Kumar, V., and Panda, D. (2007) A membrane protein, EzrA, regulates assembly dynamics of FtsZ by interacting with the C-terminal tail of FtsZ. *Biochemistry 46*, 11013−11022.

(12) Singh, J. K., Makde, R. D., Kumar, V., and Panda, D. (2008) SepF increases the assembly and bundling of FtsZ polymers and stabilizes FtsZ protofilaments by binding along its length. *J. Biol. Chem. 283*, 31116−31124.

(13) Cabeen, M. T., and Jacobs-Wagner, C. (2010) The bacterial cytoskeleton. *Annu. Rev. Genet. 44*, 365−392.

(14) Handler, A. A., Lim, J. E., and Losick, R. (2008) Peptide inhibitor of cytokinesis during sporulation in *Bacillus subtilis*. *Mol. Microbiol. 68*, 588−599.

(15) Singh, P., Jindal, B., Surolia, A., and Panda, D. (2012) A rhodanine derivative CCR-11 inhibits bacterial proliferation by inhibiting the assembly and GTPase activity of FtsZ. *Biochemistry 51*, 5434−5442.

(16) Bradford, M. M. (1976) A rapid and sensitive method for the quantitation of microgram quantities of protein utilizing the principle of protein-dye binding. *Anal. Biochem. 72*, 248−254.

(17) Lu, C., Stricker, J., and Erickson, H. P. (1998) FtsZ from *Escherichia coli*, *Azotobacter vinelandii*, and *Thermotoga maritime* quantitation, GTP hydrolysis, and assembly. *Cell Motil. Cytoskeleton 40*, 71−86.

(18) Santra, M. K., and Panda, D. (2003) Detection of an intermediate during unfolding of bacterial cell division protein FtsZ: Loss of functional properties precedes the global unfolding of FtsZ. *J. Biol. Chem. 278*, 21336−21343.

(19) Tnimov, Z., Guo, Z., Gambin, Y., Nguyen, U. T., Wu, Y. W., Abankwa, D., Stigter, A., Collins, B. M., Waldmann, H., Goody, R. S., and Alexandrov, K. (2012) Quantitative analysis of prenylated RhoA interaction with its chaperone, RhoGDI. *J. Biol. Chem. 287*, 26549−26562.

(20) Mukherjee, A., and Lutkenhaus, J. (1999) Analysis of FtsZ assembly by light scattering and determination of the role of divalent metal cations. *J. Bacteriol. 181*, 823−832.

(21) Jaiswal, R., and Panda, D. (2008) Cysteine 155 plays an important role in the assembly of *Mycobacterium tuberculosis* FtsZ. *Protein Sci. 17*, 846−854.

(22) Cheng, Y., and Prusoff, W. H. (1973) Relationship between the inhibition constant (KI) and the concentration of inhibitor which causes 50% inhibition (I50) of an enzymatic reaction. *Biochem. Pharmacol. 23*, 3099−3108.

(23) Motulsky, H. J. (1999) *Analyzing Data with Graph Pad Prism*, Graph Pad Software Inc., San Diego.

(24) Jaiswal, R., Beuria, T. K., Mohan, R., Mahajan, S. K., and Panda, D. (2007) Totarol inhibits bacterial cytokinesis by perturbing the assembly dynamics of FtsZ. *Biochemistry 46*, 4211−4220.

(25) Geladopoulos, T. P., Sotiroudis, T. G., and Evangelopoulos, A. E. (1991) A malachite green colorimetric assay for protein phosphatase activity. *Anal. Biochem. 192*, 112−116.

(26) Beuria, T. K., Santra, M. K., and Panda, D. (2005) Sanguinarine blocks cytokinesis in bacteria by inhibiting FtsZ assembly and bundling. *Biochemistry 44*, 16584−16593.

(27) Shen, B., and Lutkenhaus, J. (2009) The conserved C-terminal tail of FtsZ is required for the septal localization and division inhibitory activity of MinC(C)/MinD. *Mol. Microbiol. 2*, 410−424.

(28) Buske, P. J., and Levin, P. A. (2012) The extreme C-terminus of the bacterial cytoskeletal protein FtsZ plays a fundamental role in assembly independent of modulatory proteins. *J. Biol. Chem. 287*, 10945−10957.

(29) Ray Chaudhuri, D., and Park, J. T. (1992) *Escherichia coli* cell-division gene *ftsz* encodes a novel GTP-binding protein. *Nature 359*, 251−254.

(30) Mukherjee, A., Santra, M. K., Beuria, T. K., and Panda, D. (2005) A natural osmolyte trimethylamine N-oxide promotes assembly and bundling of the bacterial cell division protein, FtsZ and counteracts the denaturing effects of urea. *FEBS J. 272*, 2760−2772.

(31) Mukherjee, A., Dai, K., and Lutkenhaus, J. (1993) *Escherichia coli* cell division protein FtsZ is a guanine nucleotide binding protein. *Proc. Natl. Acad. Sci. U.S.A. 90*, 1053−1057.

(32) Erickson, H. P. (1995) FtsZ, a prokaryotic homolog of tubulin. *Cell 80*, 367−370.

(33) Michie, K. A., and Lowe, J. (2006) Dynamic filaments of the bacterial cytoskeleton. *Annu. Rev. Biochem. 75*, 467−492.

(34) Clément, M. J., Kuoch, B. T., Ha-Duong, T., Joshi, V., Hamon, L., Toma, F., Curmi, P. A., and Savarin, P. (2009) The stathmin-derived I19L peptide interacts with FtsZ and alters its bundling. *Biochemistry 48*, 9734−9744.

(35) Michie, K. A., Monahan, L. G., Beech, P. L., and Harry, E. J. (2006) Trapping of a spiral-like intermediate of the bacterial cytokinetic protein FtsZ. *J. Bacteriol. 188*, 1680−1690.

(36) Oliva, M. A., Cordell, S. C., and Löwe, J. (2004) Structural insights into FtsZ protofilament formation. *Nat. Struct. Mol. Biol. 11*, 1243−1250.
(37) Huecas, S., Schaffner-Barbero, C., García, W., Yébenes, H., Palacios, J. M., Díaz, J. F., Menéndez, M., and Andreu, J. M. (2007) The interactions of cell division protein FtsZ with guanine nucleotides. *J. Biol. Chem. 282*, 37515−37528.
(38) Huang, J., Cao, C., and Lutkenhaus, J. (1996) Interaction between FtsZ and inhibitors of cell division. *J. Bacteriol. 178*, 5080−5085.
(39) Schaffner-Barbero, C., Gil-Redondo, R., Ruiz-Avila, L. B., Huecas, S., Läppchen, T., den Blaauwen, T., Diaz, J. F., Morreale, A., and Andreu, J. M. (2010) Insights into nucleotide recognition by cell division protein FtsZ from a mant-GTP competition assay and molecular dynamics. *Biochemistry 49*, 10458−10472.
(40) Schaffner-Barbero, C., Martín-Fontecha, M., Chacón, P., and Andreu, J. M. (2012) Targeting the assembly of bacterial cell division protein FtsZ with small molecules. *ACS Chem. Biol. 7*, 269−277.
(41) Hritz, J., Läppchen, T., and Oostenbrink, C. (2010) Calculations of binding affinity between C8-substituted GTP analogs and the bacterial cell-division protein FtsZ. *Eur. Biophys. J. 39*, 1573−1580.
(42) Lopez, J. M., Marks, C. L., and Freese, E. (1979) The decrease of guanine nucleotides initiates sporulation of *Bacillus subtilis*. *Biochim. Biophys. Acta 587*, 238−252.